**This is an electronic reprint of the original article.**
**This reprint *may differ* from the original in pagination and typographic detail.**

**Author(s):** Napari, Mari; Malm, Jari; Lehto, Roope; Julin, Jaakko; Arstila, Kai; Sajavaara, Timo; Lahtinen, Manu

**Title:** Nucleation and growth of ZnO on PMMA by low-temperature atomic layer deposition

**Year:** 2015

**Version:**

**Please cite the original version:**

Napari, M., Malm, J., Lehto, R., Julin, J., Arstila, K., Sajavaara, T., & Lahtinen, M. (2015). Nucleation and growth of ZnO on PMMA by low-temperature atomic layer deposition. Journal of Vacuum Science and Technology A, 33(1), Article 01A128. https://doi.org/10.1116/1.4902326

All material supplied via JYX is protected by copyright and other intellectual property rights, and duplication or sale of all or part of any of the repository collections is not permitted, except that material may be duplicated by you for your research use or educational purposes in electronic or print form. You must obtain permission for any other use. Electronic or print copies may not be offered, whether for sale or otherwise to anyone who is not an authorised user.

# Nucleation and growth of ZnO on PMMA by low-temperature atomic layer deposition

Mari Napari, Jari Malm, Roope Lehto, Jaakko Julin, Kai Arstila, Timo Sajavaara, and Manu Lahtinen

Citation: Journal of Vacuum Science & Technology A **33**, 01A128 (2015); doi: 10.1116/1.4902326
View online: http://dx.doi.org/10.1116/1.4902326
View Table of Contents: http://scitation.aip.org/content/avs/journal/jvsta/33/1?ver=pdfcov
Published by the AVS: Science & Technology of Materials, Interfaces, and Processing

**Articles you may be interested in**
Functional properties of ZnO films prepared by thermal oxidation of metallic films
J. Appl. Phys. **113**, 234506 (2013); 10.1063/1.4811357

ZnO deposition on metal substrates: Relating fabrication, morphology, and wettability
J. Appl. Phys. **113**, 184905 (2013); 10.1063/1.4803553

Radical modification of the wetting behavior of textiles coated with ZnO thin films and nanoparticles when changing the ambient pressure in the pulsed laser deposition process
J. Appl. Phys. **110**, 064321 (2011); 10.1063/1.3639297

Evolution of the electrical and structural properties during the growth of Al doped ZnO films by remote plasma-enhanced metalorganic chemical vapor deposition
J. Appl. Phys. **102**, 043709 (2007); 10.1063/1.2772569

Er-doped ZnO thin films grown by pulsed-laser deposition
J. Appl. Phys. **97**, 054905 (2005); 10.1063/1.1858058

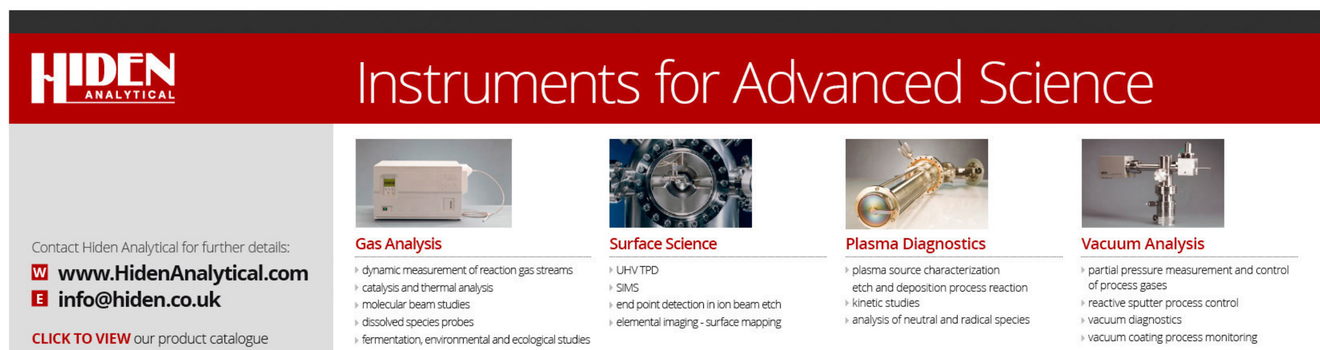


Redistribution subject to AVS license or copyright; see http://scitation.aip.org/termsconditions. Download to IP: 130.234.74.40 On: Thu, 11 Dec 2014 14:38:26

# Nucleation and growth of ZnO on PMMA by low-temperature atomic layer deposition

Mari Napari,[a)] Jari Malm, Roope Lehto, Jaakko Julin, Kai Arstila, and Timo Sajavaara
*Department of Physics, University of Jyväskylä, P.O. Box 35, FI-40014 Jyväskylä, Finland*

Manu Lahtinen
*Department of Chemistry, University of Jyväskylä, P.O. Box 35, FI-40014 Jyväskylä, Finland*

(Received 29 August 2014; accepted 10 November 2014; published 19 November 2014)

ZnO films were grown by atomic layer deposition at 35 °C on poly(methyl methacrylate) substrates using diethylzinc and water precursors. The film growth, morphology, and crystallinity were studied using Rutherford backscattering spectrometry, time-of-flight elastic recoil detection analysis, atomic force microscopy, scanning electron microscopy, and x-ray diffraction. The uniform film growth was reached after several hundreds of deposition cycles, preceded by the precursor penetration into the porous bulk and island-type growth. After the full surface coverage, the ZnO films were stoichiometric, and consisted of large grains (diameter 30 nm) with a film surface roughness up to 6 nm (RMS). The introduction of $Al_2O_3$ seed layer enhanced the initial ZnO growth substantially and changed the surface morphology as well as the crystallinity of the deposited ZnO films. Furthermore, the water contact angles of the ZnO films were measured, and upon ultraviolet illumination, the ZnO films on all the substrates became hydrophilic, independent of the film crystallinity. © *2014 American Vacuum Society*. [http://dx.doi.org/10.1116/1.4902326]

## I. INTRODUCTION

The characteristics of polymers, such as lightness, resilience and flexibility, transparency, and ease of processing give advantages in applications varying from domestic items and packaging to highly sophisticated microfabricated devices. Synthetic thermoplastic poly(methyl methacrylate) (PMMA) is one of the most applicable of amorphous polymers. Due to its transparency, it is used in optical and optoelectronic applications.[1] It is also widely used material in microelectromechanical systems.[2,3] PMMA is biocompatible and can therefore be used in medical applications, e.g., in tissue engineering and microfluidic lab-on-chip devices.[4,5] The performance of the polymer in these applications can further be improved by introducing surface engineering, such as functionalized thin film coatings.[6]

One of the interesting coating materials is zinc oxide (ZnO). ZnO is a semiconducting oxide with a wide band gap of 3.37 eV, and it has many advantageous properties, such as thermal and electrical stabilities and optical transparency.[7,8] Having antibacterial and barrier characteristics, ZnO thin films can be applied in food packaging[9,10] and also be used in catalytic applications and surface wetting adjustment due to the photoactivity of ZnO.[11] The possibility to reversibly control the surface wettability from hydrophobic to hydrophilic is especially interesting in applications such as liquid transportation in microfluidic devices.[12]

The temperature sensitivity of most polymers sets limits to the surface modification by thin film deposition.[13,14] Atomic layer deposition (ALD) is a technique for producing thin films based on repeated cycles of self-limiting gas–solid surface reactions.[15,16] Though in vacuum environment the deposition temperature is not necessarily limited to the normal operation temperatures of the polymers, the lowest possible deposition temperatures come into question in applications where the other polymer properties, such as glass transition and thermal expansion, can affect the resulting thin film quality. This is especially important in the cases of micro- and nanostructuring of the polymers, in which ALD is an otherwise superior method due to the conformal film growth. As a drawback, lower deposition temperatures require longer deposition times due to the lower reactivity of the precursors and longer purge times between the precursor pulses. Low-temperature deposition can also lead to an increased amount of impurities in the film.[17] Plasma-enhanced atomic layer deposition has been considered as a possibility to lower the substrate temperature without increasing the deposition time, but in the case of polymers, the ion bombardment and electromagnetic radiation of the plasma can cause damage to the substrate.[18]

The most common ALD process for ZnO uses diethylzinc (DEZ) and water precursors.[15] DEZ has high vapor pressure and reactivity with water, and the process is stable at temperatures even as low as room temperature; thus, ALD can be used to produce good quality ZnO thin films for polymers and other temperature sensitive substrates.[10,19,20] The ALD growth on polymers is strongly dependent on the nature of the polymer and on the ALD precursors.[11,21] For some polymers, reactive sites that can covalently bind the reactants at the initial stages of deposition are not available and the deposition initiates only after a certain number of cycles.[22] Many polymers are permeable to small molecules, which allow the diffusion of the precursors into the bulk. It has been shown that in one of the most studied processes, ALD $Al_2O_3$ using trimethylaluminum (TMA) and water, TMA diffuses into the subsurface region of the polymer where it is kinetically trapped and reacts further with water either beneath or at the surface to form nuclei. The extent of the

[a)]Electronic mail: mari.napari@jyu.fi



Redistribution subject to AVS license or copyright; see http://scitation.aip.org/termsconditions. Download to IP: 130.234.74.40 On: Thu, 11 Dec 2014 14:38:26

diffusion and the subsurface growth is dependent on both the temperature and the exposure time of the reactant.[22] The subsurface growth affects on the structure of the polymer substrate/film interface as well as the surface roughness of the film.[21,22] Parsons *et al.*[21] introduced another possible mechanism for TMA reaction with PMMA. In this mechanism, the Lewis-acidic TMA reacts with the Lewis-basic carbonyl groups on PMMA side-chains. The reactions lead to the degradation of the PMMA and promote the precursor diffusion into the subsurface region. Similarly to the case of TMA, this reaction mechanism can govern the surface reactions with Lewis-acidic DEZ and PMMA. Having a smaller size and linear structure, the DEZ molecules may diffuse even deeper into the polymer.

In this work, ZnO films were deposited on two grades of PMMA substrates by low-temperature ALD, and the film growth and structure were analyzed with several characterization methods. On the growth studies, the emphasis was on the diffusion of the DEZ precursor and the growth-initiating subsurface nucleation during the deposition. The depositions were made on two polymer substrates that are similar in chemistry but differ in other surface properties such as porosity. Furthermore, the influence of the deposition of $Al_2O_3$ seed layer to the ZnO film growth, morphology, and crystallinity was investigated. Additionally, the photoinduced changes in the surface wetting properties of the deposited ZnO films on PMMA were studied. The reversible control of surface hydrophilicity/hydrophobicity of the ZnO films grown by ALD has applications in microfluidics, where thin functional coatings on patterned polymer platforms can be used to manipulate the fluid flows.

## II. EXPERIMENT

### A. Thin film deposition

Two types of PMMA substrates were used, 1 mm thick bulk commercial grade sheet (Evonik Plexiglas XT) and PMMA films made from e-beam resist (MicroChem MW 950 kDa 11% in Anisole), spin coated on $10 \times 10\,\mathrm{mm}^2$ silicon wafer and baked on a hot plate at 160 °C for 2 min, resulting in film thickness of 2–2.5 $\mu$m. The bulk PMMA was rinsed with isopropanol to remove the possible residues from the protective foils of the PMMA sheet. Beside the PMMA, silicon (111) was used as a reference substrate in all the depositions. The native oxide on the Si surface was not removed. ZnO films were deposited at 35 °C using Beneq TFS-200 reactor. Prior to the deposition, the polymer substrates were held in vacuum in the reactor load lock for the removal of the absorbed water from the PMMA. DEZ ($\geq$95%, Strem Chemicals Inc., and electronic grade from SAFC Hitech) and deionized water were used as precursors and nitrogen as the carrier and purge gas. The reactor pressure was 5 mbars during the depositions. The deposition cycles for ZnO were either 0.15/30/0.15/30 s or 0.3/30/0.3/30 s (DEZ/$N_2$/$H_2O$/$N_2$). Long purge times were used to ensure an efficient removal of the precursors and reaction by-products from the substrates. For the growth studies, the number of ZnO cycles varied from 100 to 800. Additionally, samples with 1600 cycles of ZnO were deposited to investigate the crystallinity of the ZnO films on PMMA. To study the effect of intermediate seed layer to the ZnO growth and film properties, $Al_2O_3$ with TMA (electronic grade from SAFC Hitech) and water precursors was deposited on PMMA substrate prior to the ZnO film under the same conditions. For $Al_2O_3$, the deposition cycle was 0.3/30/0.3/30 s (TMA/$N_2$/$H_2O$/$N_2$), and samples with 20, 50, and 100 cycles of $Al_2O_3$ intermediate layer were prepared.

### B. Characterization

The Zn areal densities in the ZnO films with and without the $Al_2O_3$ intermediate layer were determined using Rutherford backscattering spectrometry (RBS)[23] with 2.415 MeV $He^{2+}$ incident beam and 165° scattering angle and analyzed with SimNRA program.[24] The ion fluence in RBS measurements was normalized against the beam chopper and Si reference sample to gain the normalized Zn areal densities of the films. Additionally, the thicknesses of the films deposited on Si substrates were measured using optical ellipsometer (Rudolph AutoEL III). The elemental composition and film impurities were investigated using time-of-flight elastic recoil detection analysis (ToF-ERDA)[23,25] with 13.615 MeV $^{79}Br^{7+}$ ions and Potku analysis software.[26] The surface topography and morphology were studied with atomic force microscopy (AFM) (Digital Instruments, Dimension 3100 Nanoscope, Veeco Metrology Group) and scanning electron microscopy (SEM) (Raith E-line, acceleration voltage 3 kV). The ZnO crystallinity was examined by powder x-ray diffraction (XRD) (PANalytical X'Pert PRO diffractometer, Cu K$\alpha_1$; $\lambda = 1.5406$ Å, 45 kV, 40 mA) and analyzed with X'pert HighScore Plus program implemented with the ICDD PDF-4+ powder diffraction database. The water contact angles were measured using the sessile drop method. Droplets, 5 $\mu$l of deionized water, were produced using a micropipette mounted to a linear translation stage for accurate deposition. The profile of the droplet on the sample surface was imaged with a high speed camera (Redlake Motion Pro X3), and the images were analyzed with a DropSnake plugin for ImageJ program.[27,28] Frame rate of 10 frames per second was used to capture the dynamics of the wetting within the 30 s measurement time. For every measurement point, the average value of contact angles measured from 2 to 3 locations on the sample was taken. To study the UV-induced hydrophilicity, UV illumination was accomplished using 350 W UV400 Hg lamp of a Karl Suss MA45 mask aligner (i-line 365 nm peak intensity ca. 6 mW $\mathrm{cm}^{-2}$). The samples were illuminated for 15 min. Prior to the illumination, the samples were rinsed with deionized water, dried with nitrogen and kept in a dry and dark environment for 2–3 days.

## III. RESULTS AND DISCUSSION

### A. ZnO growth on PMMA

The growth per cycle of ZnO determined with ellipsometry from the deposited films on Si was ~0.8 Å/cycle, which is in agreement with the previous studies of low-temperature



Redistribution subject to AVS license or copyright; see http://scitation.aip.org/termsconditions. Download to IP: 130.234.74.40 On: Thu, 11 Dec 2014 14:38:26

ALD of ZnO.[10] The slow growth is due to the lower reactivity and incomplete surface reactions with DEZ and water.[19] As the film thicknesses on PMMA could not be directly measured due to the nonuniform growth during the first hundreds of deposition cycles, the film growth was studied by measuring the Zn areal density of the films using Rutherford backscattering spectrometry. Figure 1 shows the areal density of the Zn in the units of atoms per square centimeter as a function of ZnO deposition cycles. The surface topography of the commercial bulk PMMA (b), leading to larger surface area, was measured with AFM and it is taken into account in the normalization.

The initial growth on PMMA is slower than on the Si substrate. After 400–500 deposition cycles, the growth becomes more linear, which may indicate a full surface coverage after which the ALD growth is surface-limited. Even after the assumed full film surface coverage, the growth per cycle on Si is approximately 1.4 times higher than that observed on the PMMA substrates. The nonlinear growth of ZnO on PMMA on the first 400 cycles is assumed to be governed by the limited adsorption of DEZ onto PMMA. The differences in the growth between the PMMA substrates cannot be explained only by the AFM measured topography of the bulk PMMA, but by the differences in the nanoscale roughness and/or porosity of the two PMMA grades. It can be assumed, that the DEZ precursor diffuses more easily into the more porous bulk PMMA and is kinetically trapped. The trapped DEZ molecules can subsequently further react with water and start the subsurface nucleation. On the spin coated PMMA, the oxide formation reactions are limited on the denser surface of the substrate with less reactive sites for the DEZ adsorption, delaying the initialization of the nucleation and thus leading to the slower growth. Another explanation can be the significantly higher surface area due to the nanoscale roughness of the commercial grade material. In this case, the adsorption mechanisms of the DEZ precursor are the same for both PMMA grades, but the increase in the available adsorption sites leads to the faster ZnO growth and Zn areal density increase on bulk PMMA.

Figure 2 shows the Zn peaks from RBS spectra measured from ZnO films on different substrates after (a) 300 and (b) 800 ALD cycles. Clear differences in Zn peak widths and areas between the bulk and spin coated PMMA can be observed. In Fig. 2(b), the surface of the bulk PMMA is saturated, followed by the surface limited growth, which can be seen as similarity of the peak shapes at the film surface (higher energies). Films grown on Si are shown as references.

When deposited on the $Al_2O_3$ seed layer, the growth of ZnO is substantially enhanced compared to the direct deposition on the PMMA. This is likely due to the presence of the reactive hydroxyl groups on the $Al_2O_3$ for DEZ surface adsorption. Unlike ZnO, $Al_2O_3$ grows linearly on PMMA substrate already after 20 deposition cycles, which was verified both with the RBS and ToF-ERDA measurements. It has been reported that the nucleation stage of $Al_2O_3$ on most polymers takes only 10–20 cycles, after which the growth becomes linear.[6,22] When deposited on the aluminum oxide layer, the growth of ZnO on PMMA resembles the growth on Si substrate as shown in Fig. 3, and there is no difference between the ZnO film deposited on the bulk PMMA with $Al_2O_3$ layer and the ZnO on Si with $Al_2O_3$. This indicates

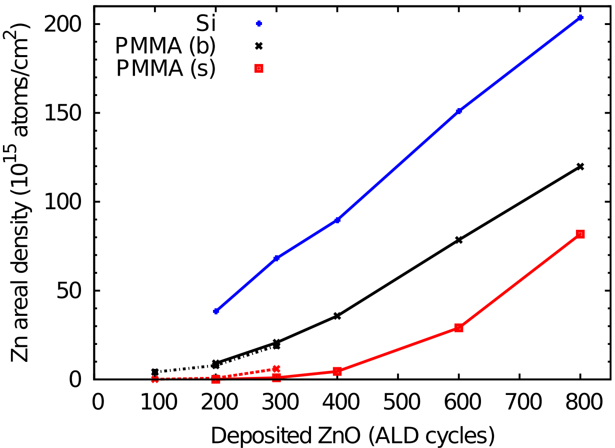


Fig. 1. (Color online) Areal density of Zn in ZnO films on Si, bulk (b) PMMA, and spin coated (s) PMMA substrates measured with RBS as a function of ZnO ALD cycles. The solid and dashed lines represent the growth on the films deposited using 0.15 and 0.30 s precursor pulses, respectively.

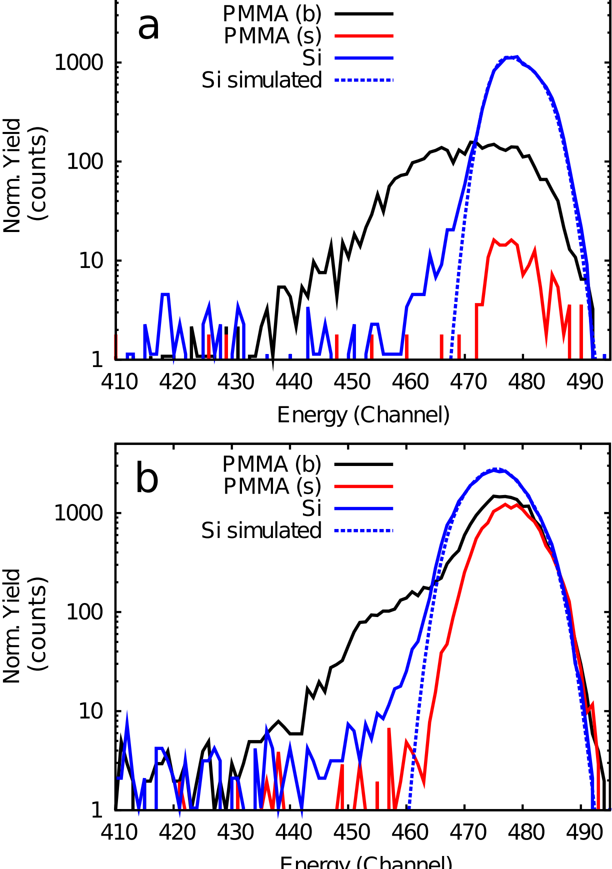


Fig. 2. (Color online) Normalized Zn peaks on RBS spectra measured from ZnO films on Si, bulk (b) PMMA, and spin coated (s) PMMA deposited with (a) 300 and (b) 800 ZnO ALD cycles. The dashed lines represent the simulated Zn peak on Si, corresponding to stoichiometric ZnO films with film thicknesses of $135 \times 10^{15}$ at./cm$^2$ (a) and $410 \times 10^{15}$ at./cm$^2$ (b).



Redistribution subject to AVS license or copyright; see http://scitation.aip.org/termsconditions. Download to IP: 130.234.74.40 On: Thu, 11 Dec 2014 14:38:26

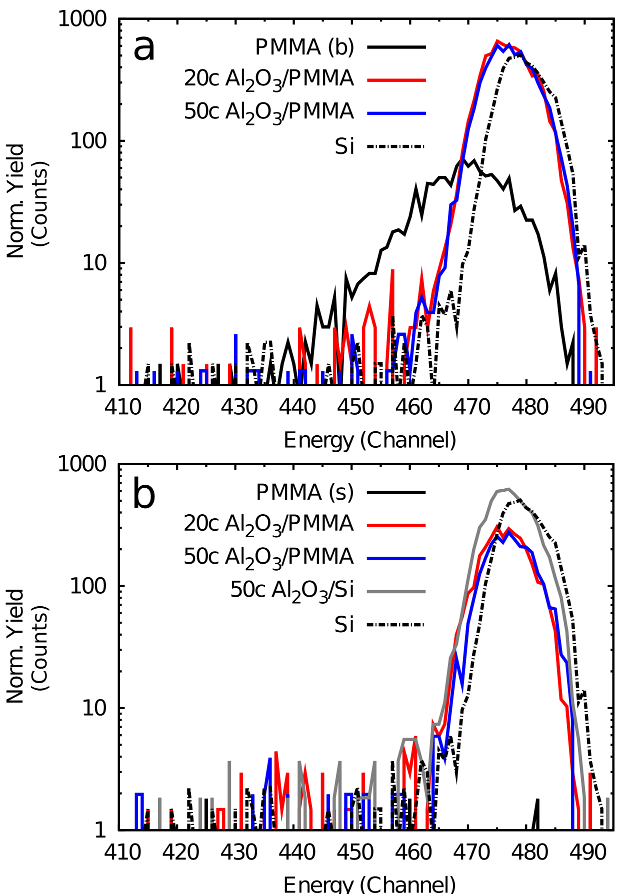


FIG. 3. (Color online) Normalized Zn peaks on RBS spectra measured from ZnO films grown by 200 ALD cycles on (a) bulk PMMA and (b) spin coated PMMA substrates either directly or with $Al_2O_3$ seed layer of different thicknesses. The dashed black line on both (a) and (b) represents the 200 cycles ZnO films deposited directly on Si, and the gray line in (b) on 50 cycles of $Al_2O_3$ on Si.

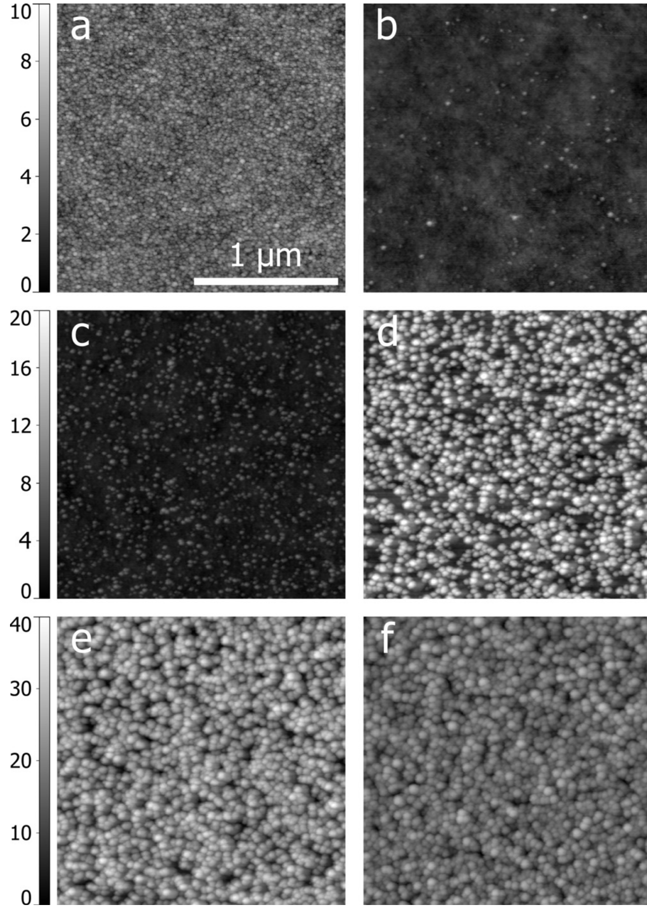


FIG. 4. AFM images of ALD ZnO films deposited at 35 °C on spin-coated PMMA substrates. (a) 200 cycles ZnO on 50 cycles $Al_2O_3$; (b) 200, (c) 300, (d) 400, (e) 600, and (f) 800 cycles of ZnO. Image area of each panel is $2 \times 2\ \mu m^2$.

that the $Al_2O_3$ layer acts as a barrier preventing the diffusion of DEZ into the polymer subsurface region. There were no differences in ZnO films deposited on $Al_2O_3$ layers with thicknesses of 20 and 50 ALD cycles. However, when deposited on the $Al_2O_3$ layers, the initial ZnO growth per cycle is lower on the spin coated PMMA than on the bulk, which can be explained by the different surface areas arising from the nanoscale porosity of the bulk PMMA substrate.

To compare the results from the RBS measurements to the film topography, the ZnO films on PMMA substrates were measured with AFM. As shown in Figs. 4(b)–4(f), the films grow on PMMA by island-type growth, which is typical for ZnO on polymer substrates.[10] After 200 cycles, only minor surface area is covered with ZnO islands (diameter 10–15 nm) and the number of islands and size increases until the diameter reaches 30 nm, after which it remains constant with increasing surface coverage. At the same time, the total film surface RMS roughness increases from 0.5 to 6.0 nm, being highest at 600 deposition cycles after which the roughness decreases to around 4 nm. After the initial nucleation, the reactions take place more readily on the ZnO grains instead of the polymer surface, which leads to the larger grain size throughout the film thickness resulting also the increased surface roughness. The increased roughness and grain size of the 800 cycles ZnO deposited directly on bulk PMMA can similarly be seen from the SEM image in Fig. 5(a).

Depositing the intermediate $Al_2O_3$ layer has an effect also on the surface topography of the ZnO film [Fig. 4(a)]. The ZnO grown on the $Al_2O_3$ layer has smaller and more uniform grain size (<10 nm) with a smoother surface, RMS roughness being 1.0 nm, which is similar to the films deposited on Si. In the films deposited on the $Al_2O_3$, the film topography also appears to be independent on the ZnO film thickness. Figure 5 shows the SEM images of the 800 ZnO cycles deposited directly on the PMMA surface and on top of the 50 cycles $Al_2O_3$ layer. The grain size and roughness are the same as with 200 cycles of ZnO on the $Al_2O_3$ as presented in Fig. 4(a).

The elemental compositions of the ALD ZnO were determined from the films deposited on the silicon substrate using ToF-ERDA. The films were close to stoichiometric composition within the measurement uncertainty. The only visible impurities were hydrogen (6 ± 1 at. %) and carbon (<0.5 at. %). The measurements on the PMMA substrates were kept short to minimize the sample damage caused by the heavy ion bombardment. On the polymer substrate, the



Redistribution subject to AVS license or copyright; see http://scitation.aip.org/termsconditions. Download to IP: 130.234.74.40 On: Thu, 11 Dec 2014 14:38:26

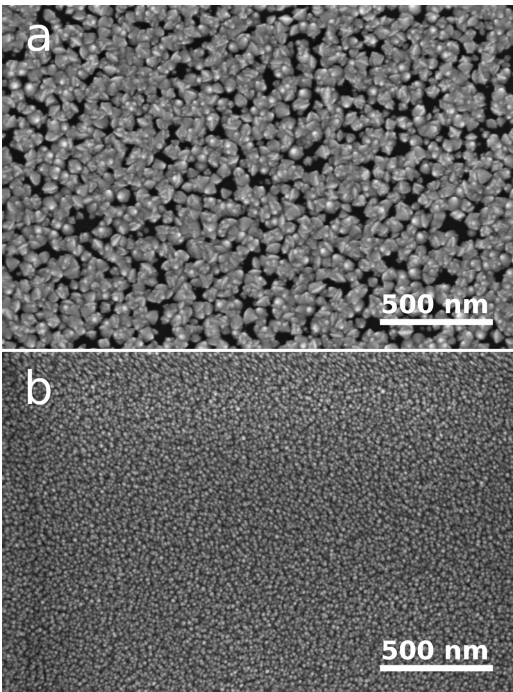


FIG. 5. Scanning electron micrographs of (a) 800 cycles of ZnO deposited on PMMA substrate and (b) 800 cycles of ZnO deposited on 50 cycles $Al_2O_3$ intermediate layer between the PMMA and ZnO film.

analysis of the film composition is hampered by the diffusion of the precursors into the bulk during the deposition as well as by the migration of the light elements into the film from the substrate during the measurement, both increasing the uncertainty of the analysis. The ZnO film composition was measured with the 50 cycles $Al_2O_3$ intermediate layer, on which the composition of ZnO film on the PMMA substrates were comparable with the films deposited on silicon. This confirms the role of $Al_2O_3$ as a barrier layer preventing the DEZ diffusion during ALD. Figures 6(a) and 6(b) show the ToF-ERDA depth profiles of 800 cycles of ZnO deposited on 50 cycles of $Al_2O_3$ on spin coated and bulk PMMA, respectively.

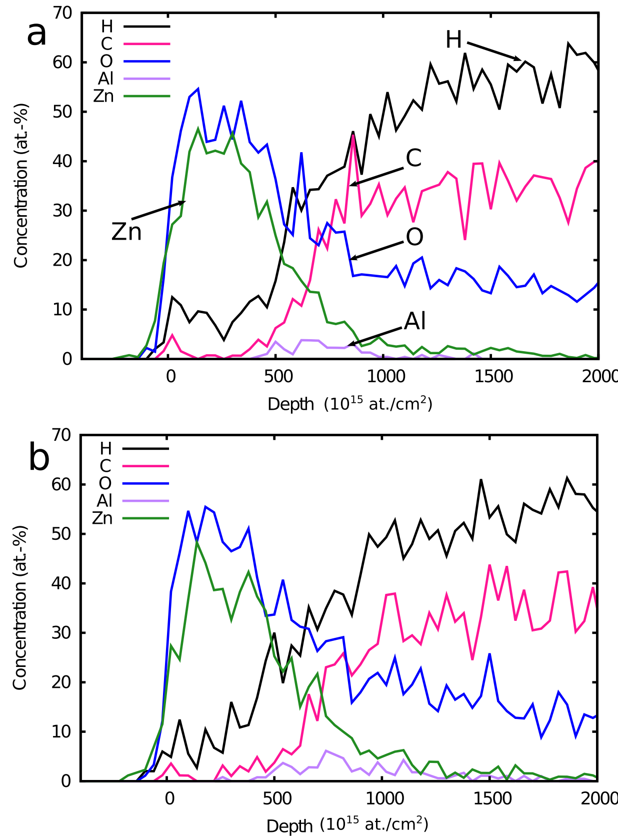


FIG. 6. (Color online) ToF-ERDA depth profiles of 800 cycles of ZnO on top of 50 cycles of $Al_2O_3$ on (a) spin coated PMMA and (b) bulk PMMA substrate.

## B. Crystallinity

The polycrystalline growth of ALD ZnO at low temperatures on Si has been previously reported by Malm *et al.*[19] According to their study, the crystal orientation of the films is strongly deposition temperature dependent, being hexagonal (002) dominant at temperatures below 70 °C, with the c-axis perpendicular to the substrate surface. However, the crystallinity of ZnO at low temperatures depends also on the film growth rate and the substrate. Deposited at 35 °C, the ZnO on silicon substrate was found to be partially crystalline with c-axis orientation, which in agreement with the previous studies. When grown on the PMMA substrate, the ZnO film was amorphous even after 800 deposition cycles with almost no indication of crystal orientation, despite the grain structure of the film, as shown in Fig. 7. When the number of deposition cycles is increased to 1600, the strong hexagonal (002) diffraction peak can be identified in the XRD pattern together with the low intensity (100) peak. When deposited on $Al_2O_3$ intermediate layer, the ZnO films showed some degree of hexagonal crystal orientation already after 800 deposition cycles, but the intensity of the visible (002)

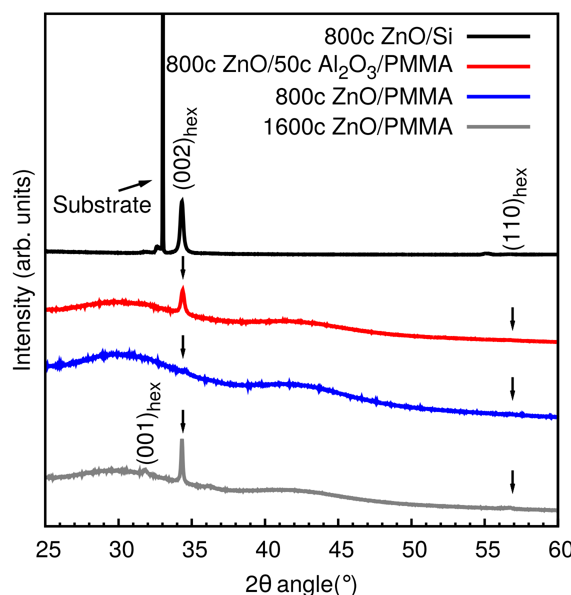


FIG. 7. (Color online) XRD patterns of 800 cycles of ZnO deposited on Si and bulk PMMA substrates with and without $Al_2O_3$ intermediate layer, and an XRD pattern of 1600 cycles ZnO film on bulk PMMA.



Redistribution subject to AVS license or copyright; see http://scitation.aip.org/termsconditions. Download to IP: 130.234.74.40 On: Thu, 11 Dec 2014 14:38:26

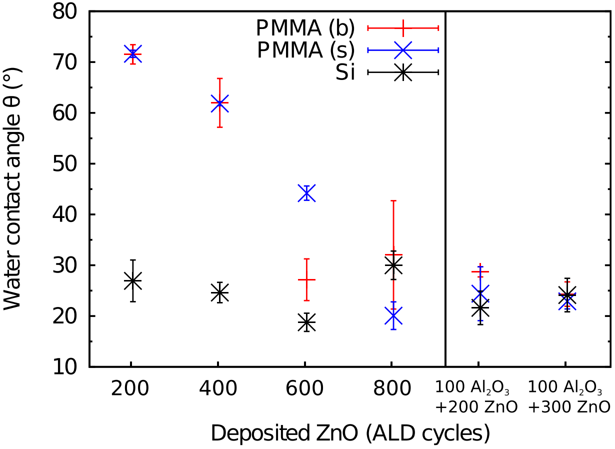


FIG. 8. (Color online) Water contact angles ($\theta$) of UV-illuminated ZnO deposited on spin coated PMMA (s), bulk PMMA (b), and Si substrates as a function of ZnO ALD cycles. Two rightmost points represent the contact angles of ZnO deposited on 100 cycles $Al_2O_3$ intermediate layer.

diffraction peak is lower compared to the diffraction peaks arising from the ZnO films deposited on the Si substrate.

### C. Wetting

The hydrophilicity of ZnO coated PMMA was studied using water contact angle measurements. As-deposited ZnO is hydrophobic, having a contact angle of 110° on Si. On PMMA, there was more variation on as-deposited films due to the surface roughness, contact angle being 75° on average. The contact angle is significantly reduced by UV exposure. On films deposited on Si substrate, the contact angle is approximately constant at ca. 25° after the illumination, independently of the film thickness. On PMMA, the contact angle decreases with increasing film coverage, from the 71° of the native PMMA to 25°, as shown in Fig. 8. The water contact angle is somewhat affected by the ZnO film roughness, causing local variations to the values measured within the same sample. When the ZnO is deposited on the $Al_2O_3$ intermediate layer, the water contact angle is independent on the used substrate. No changes in the contact angles were detected within the measurement time, which indicates the stability of the ZnO surface when in contact with water. The reversible photoinduced changes in the wettability of semiconducting oxides, $TiO_2$ and ZnO, is typically realized on crystalline films.[12] As shown in Fig. 7, the films on PMMA substrates grow amorphous, possessing still the same properties as the more crystalline ZnO deposited on crystalline substrates. Though no photoinduced superhydrophilicity was achieved with used illumination doses, the water contact angles of the films decreased on the polymer surfaces. This gives a possibility to surface wettability control which can be used, e.g., in analytical applications and microfluidics by fabricating hydrophilic flow channels by masked UV illumination.

## IV. CONCLUSIONS

Zinc oxide thin films using diethyl zinc and water precursors can be grown at low deposition temperatures on PMMA. At 35 °C, the uniform film growth is initialized after several hundred of deposition cycles, preceded by island-type growth. There was a clear difference in growth on two types of PMMA used in the study. When deposited on bulk PMMA, the DEZ precursor penetrates into the porous polymer initializing the subsurface nucleation, which was not observed in the case of the spin coated PMMA substrates. After full film coverage, the resulting films had rough topography with large grain structure. On Si, ZnO grew as polycrystalline film, whereas on PMMA, the film crystallinity was strongly dependent on the film thickness. The growth was substantially enhanced by introducing an $Al_2O_3$ intermediate seed layer between the polymer substrate and the ZnO film. The results show that even a thin $Al_2O_3$ layer acts as a barrier against precursor diffusion into the polymer, and changes the surface topography as well as the crystallinity of the ZnO films grown by ALD. The ZnO surfaces showed degreasing water contact angles upon UV illumination on both Si and PMMA, independent of the film crystallinity. This enables the controlling of wettability of PMMA surfaces by ZnO thin film deposition.

## ACKNOWLEDGMENTS

This work was supported by European Union—European Regional Development Fund via NANOPALVA-Project (A32219), Academy of Finland Center of Excellence in Nuclear and Accelerator Based Physics (Ref. No. 251353), and the Doctoral Programme in Nuclear and Particle Physics (PANU, University of Jyväskylä).

[1]U. Schulz and N. Kaiser, Prog. Surf. Sci. **81**, 387 (2006).
[2]N.-C. Tsai and C.-Y. Sue, Sens. Actuators, A **134**, 555 (2007).
[3]A. C. Henry, T. J. Tutt, M. Galloway, Y. Y. Davidson, C. S. McWhorter, S. A. Soper, and R. L. McCarley, Anal. Chem. **72**, 5331 (2000).
[4]A. E. Guber *et al.*, Chem. Eng. J. **101**, 447 (2004).
[5]P. Abgrall and A.-M. Gué, J. Micromech. Microeng. **17**, R15 (2007).
[6]M. Kemell, E. Färm, M. Ritala, and M. Leskelä, Eur. Polym. J. **44**, 3564 (2008).
[7]A. W. Ott and R. P. H. Chang, Mater. Chem. Phys. **58**, 132 (1998).
[8]I. A. Kowalik, E. Guziewicz, K. Kopalko, S. Yatsunenko, A. Wójcik-Głodowska, M. Godlewski, P. Dłużewski, E. Łusakowska, and W. Paszkowicz, J. Cryst. Growth **311**, 1096 (2009).
[9]M.-L. Kääriäinen, C. K. Weiss, S. Ritz, S. Pütz, D. C. Cameron, V. Mailänder, and K. Landfester, Appl. Surf. Sci. **287**, 375 (2013).
[10]M. Vähä-Nissi *et al*, Thin Solid Films **562**, 331 (2014).
[11]A. K. Roy, D. Deduytsche, and C. Detavernier, J. Vac. Sci. Technol., A **31**, 01A147 (2013).
[12]V. Kekkonen, A. Hakola, T. Kajava, E. Sahramo, J. Malm, M. Karppinen, and R. H. A. Ras, Appl. Phys. Lett. **97**, 044102 (2010).
[13]J. Nikkola, J. Sievänen, M. Raulio, J. Wei, J. Vuorinen, and C. Y. Tang, J. Membr. Sci. **450**, 174 (2013).
[14]M. Vähä-Nissi, J. Sievänen, E. Salo, P. Heikkilä, E. Kenttä, L.-S. Johansson, J. T. Koskinen, and A. Harlin, J. Solid State Chem. **214**, 7 (2013).
[15]V. Miikkulainen, M. Leskelä, M. Ritala, and R. L. Puurunen, J. Appl. Phys. **113**, 021301 (2013).
[16]R. L. Puurunen, J. Appl. Phys. **97**, 121301 (2005).
[17]O. M. E. Ylivaara *et al.*, Thin Solid Films **553**, 124 (2014).
[18]T. O. Kääriäinen, D. C. Cameron, and M. Tanttari, Plasma Processes Polym. **6**, 631 (2009).
[19]J. Malm, E. Sahramo, J. Perälä, T. Sajavaara, and M. Karppinen, Thin Solid Films **519**, 5319 (2011).



Redistribution subject to AVS license or copyright; see http://scitation.aip.org/termsconditions. Download to IP: 130.234.74.40 On: Thu, 11 Dec 2014 14:38:26

[20]J. Malm, E. Sahramo, M. Karppinen, and R. H. A. Ras, Chem. Mater. **22**, 3349 (2010).
[21]G. N. Parsons *et al*., Coord. Chem. Rev. **257**, 3323 (2013).
[22]C. A. Wilson, R. K. Grubbs, and S. M. George, Chem. Mater. **17**, 5625 (2005).
[23]M. Putkonen, T. Sajavaara, L. Niinistö, and J. Keinonen, Anal. Bioanal. Chem. **382**, 1791 (2005).
[24]M. Mayer, AIP Conf. Proc. **475**, 541 (1999).
[25]M. Laitinen, M. Rossi, J. Julin, and T. Sajavaara, Nucl. Instrum. Methods, B **337**, 55 (2014).
[26]K. Arstila *et al*., Nucl. Instrum. Methods, B **331**, 34 (2014).
[27]M. D. Abràmoff, P. J. Magalhães, and S. J. Ram, Biophotonics Int. **11**, 36 (2004).
[28]A. F. Stalder, G. Kulik, D. Sage, L. Barbieri, and P. Hoffmann, Colloids Surf., A **286**, 92 (2006).



Redistribution subject to AVS license or copyright; see http://scitation.aip.org/termsconditions. Download to IP: 130.234.74.40 On: Thu, 11 Dec 2014 14:38:26